1P2-10

Application of spatial spectral entropy on composite materials for noncontact acoustic inspection

非接触音響探査法のための空間スペクトルエントロピーの複合材料への適用

Kazuko Sugimoto[1†], Tsuneyoshi Sugimoto[1], Noriyuki Utagawa[2] and Chitose Kuroda[2]
([1]Grad. School Eng., Toin Univ. of Yokohama; [2]SatoKogyo Co., Ltd.)
杉本和子 [1†]，杉本恒美 [1]，歌川紀之 [2]，黒田千歳 [2] ([1] 桐蔭横浜大学院　工, [2] 佐藤工業㈱技術研究所)

1. Introduction

In a non-destructive manner, noncontact acoustic inspection method can detect and visualized internal defects (crack, peeling, cavity, etc.) in shallow layer of composite material such as concrete from a long distance[1-3]. A two-dimensional vibration velocity distribution is measured using a planar acoustic excitation and a scanning laser Doppler vibrometer (SLDV). When there is an internal defect, a flexural resonance occurs in a defective part, and vibration energy difference from a healthy part can be detected and imaged as vibrational energy ratio. If the resonance frequency range of internal defect is known, a clear acoustic image can be generated by narrowing the analysis frequency range rather than the entire measured frequency range. The resonance frequency due to internal defects appeared in a measurement plane can be detected by 'spatial spectral entropy (SSE)' [4] we proposed before. Verification was performed using circular peeling defects with various sizes and burial depths.

2. Experimental setup

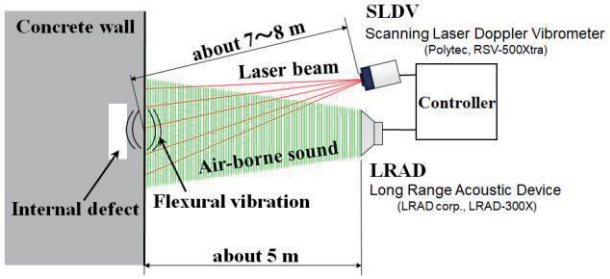

Fig. 1　Experimental setup.

Fig. 1 shows the experimental setup. In order to detect Internal defects, strong plane waves were irradiated from a long-range acoustic device (LRAD; LRAD corp., LRAD-300X) installed at a distance of about 5 m from the measurement plane, and the concrete measurement surface was acoustically excited. A scanning laser Doppler vibrometer (SLDV; Polytec, RSV-500Xtra scanning vibrometer) was installed at a distance of 5-7 m from the measurement surface, and the two-dimensional vibration velocity distribution on the measurement plane was measured. After time-frequency gate processing to reduce noise from surroundings, vibration velocity spectrum was calculated.

[†]kazukosu@toin.ac.jp

3. Spatial Spectral Entropy (SSE)

SSE can detect not only the resonance frequency of internal defects but also the resonance frequency of a laser head of SLDV. SSE was defined by the following equation.

$$H_{SSE}(f) = -\sum_{i=1}^{m}\sum_{j=1}^{n} P_{i,j}(f)\, log_2\, P_{i,j}\,(f) \qquad (1)$$

$$P_{i,j}(f) = \frac{S_{i,j}(f)}{\sum_{i=1}^{m}\sum_{j=1}^{n} S_{i,j}(f)}$$

Where $H_{SSE}(f)$ is spectral entropy extended to real space. $S_{i,j}(f)$ is the frequency component of power spectrum of vibration velocity at each measurement point$r_{i,j}$. $P_{i,j}(f)$ is probability that $S_{i,j}(f)$ exists in the measured plane. Therefore, $H_{SSE}(f)$ indicates the information entropy calculated for the frequency component f of vibration velocity spectrum at all measured points.

4. Experimental Results

Peeling defects are more difficult to detect than the same size of cavity defects. **Fig. 2** shows the shape, size, and burial depth of peeling defects that we investigated.

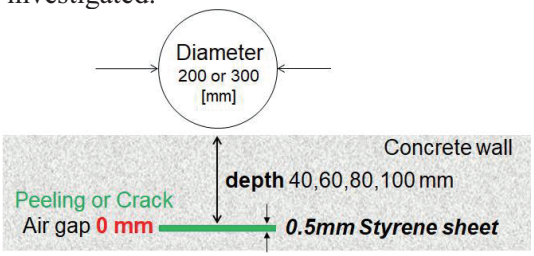

Fig. 2　Position and size of a circular peeling defect embedded in concrete wall specimen.

As an example of experimental results, a circular peeling defect (diameter 300 mm, burial depth 60 mm) is shown below. **Fig. 3** shows a result of SSE analysis. A resonance peak due to internal defect is observed in the frequency range 2550-2850 Hz in red frame. The black dotted line in the figure

is the median of SSE value, 5.71, calculated in the measurement frequency range (1000-4800 Hz).

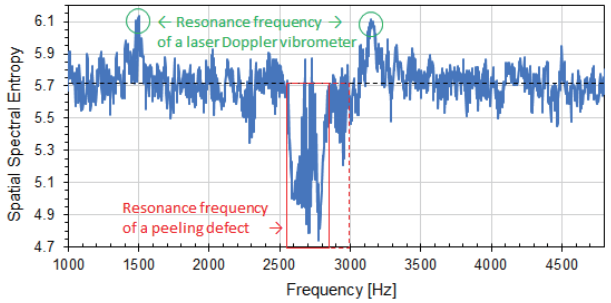

Fig. 3 Analysis result by spatial spectral entropy (SSE).

Fig. 4 is an acoustic image of a circular peeling defect. The frequency range for imaging of (a) was 1000-4800 Hz, and that of (b) was 2550-2850Hz. Based on the SSE result, vibrational energy ratio was calculated in a narrower frequency range and (b) was visualized.

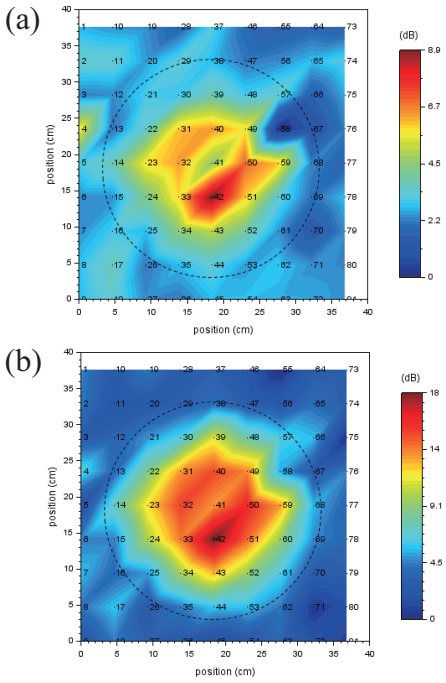

Fig. 4 Acoustic defect image of circular peeling defect (Φ300, 60) by vibrational energy ratio, Frequency band for imaging (a)1000-4800Hz, (b)2550-2850Hz.

In our noncontact acoustic inspection method, flexural resonance is appeared as a vibration state due to defect such as a cavity or a peeling. As the theoretical formula of flexural resonance of a solid circular plate (clamped all around or simply supported all around), the natural frequency is known as

$$f_{mn} = \frac{1}{2\pi}\frac{\lambda_{mn}}{a^2}\sqrt{\frac{Eh^2}{12(1-\nu^2)\rho}} \qquad (2)$$

where f_{mn}: natural frequency [Hz], E: Young's modulus [Pa], a: radius of disk [m], ρ: mass per unit volume [kg/m^3], h: plate thickness [m], ν: Poisson's ratio, m: number of nodal circles, n: number of nodal diameters.

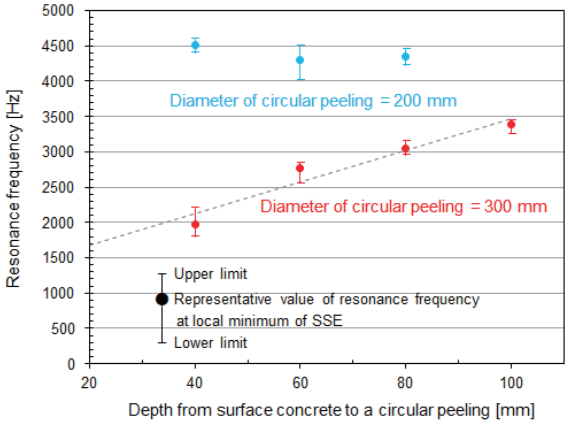

Fig. 5 Relation between resonance frequency of circular peeling defect and diameter or burial depth.

Fig. 5 was plotted the resonance frequency due to defect against burial depth for each circular peeling defect. For a circular peeling defect with 300 mm diameter, the resonance frequency increased proportionally as burial depth increased at 40-100 mm. It can also be seen that the resonance frequency increases as the defect size decreases. This is a phenomenon estimated from Equation (2). If the concrete measurement surface can be acoustically excited enough, the phenomenon of flexural resonance may be able to be caught. These phenomena were fitted to the theoretical formula of flexural resonance of a flat disk.

5. Conclusion

The noncontact acoustic inspection method can detect the resonance frequency of the measured surface and their frequency range by spatial spectral entropy (SSE) analysis using vibration velocity data measured remotely. Once the resonance frequency of defect was known, the acoustic image of peel defect was clearly visualized by narrowing the imaging frequency range. In addition, for circular peeling defects used in this experiment, phenomena that fit the theoretical equation of flexural resonance were observed.

References

1. K. Katakura, R. Akamatsu, T. Sugimoto and N. Utagawa: Jpn. J. Appl. Phys. **53** (2014) 07KC15.
2. K. Sugimoto, R. Akamatsu, T. Sugimoto, N. Utagawa, C. Kuroda and K. Katakura: Jpn. J. Appl. Phys. **54** (2015) 07HC15.
3. K. Sugimoto, T. Sugimoto, N. Utagawa, C. Kuroda and A. Kawakami: Jpn. J. Appl. Phys. **57** (2018) 07LC13.
4. K. Sugimoto, T. Sugimoto, N. Utagawa and C. Kuroda: Jpn. J. Appl. Phys. **58** (2019) SGGB15.